Systematic Study of the $^{88}Sr(^{16}O, ^{15}N)$ Reaction*

N. Anantaraman†‡
Argonne National Laboratory, Argonne, Illinois 60439, and University of Chicago, Chicago, Illinois 60637

(Received 9 July 1973)

The systematics of the $^{88}Sr(^{16}O, ^{15}N)$ one-proton transfer reaction is investigated for six incident energies between 44.0 and 59.0 MeV. Angular distributions for the prominent transitions are presented. Finite-range no-recoil calculations with optical-model parameters determined from the elastic scattering of ^{16}O on ^{88}Sr and of ^{15}N on ^{89}Y fit the transfer angular distributions well, except for transitions involving large Q mismatch. The energy-dependent normalization obtained for the transition to the $2p_{1/2}$ state indicates the increasing importance of recoil contributions at higher incident energies. A semiclassical treatment of the transfer reaction seems to be adequate at incident energies below the Coulomb barrier.

[NUCLEAR REACTIONS $^{88}Sr(^{16}O, ^{15}N)$, $^{88}Sr(^{16}O, C)$, $^{88}Sr(^{16}O, ^{16}O)$ $E = 44-59$ MeV measured $\sigma(E, \theta)$; deduced optical-model parameters. Enriched target, DWBA analysis, resolution 400 keV, $\theta = 60°-160°$.]

I. INTRODUCTION

There are many recent studies of one-nucleon transfer reactions induced by heavy ions on a variety of targets at bombarding energies both in the vicinity of the Coulomb barrier[1-3] and at much higher energies.[4,5] Yet there has been no systematic study of any one reaction on a single target for a range of bombarding energies. Such a study is of interest for the reasons given below.

Korner *et al.*[1] and Maher, Erb, and Miller[2] have fitted $(^{16}O, ^{15}N)$ angular distributions on fp-shell nuclei by finite-range no-recoil distorted-wave Born-approximation (DWBA) calculations.[6] Optical-model parameters for the entrance channel were taken from the analysis of elastic scattering. Since there were no data on ^{15}N elastic scattering at the time their calculations were done, the same set of parameters was taken for the exit channel, except that the diffuseness had to be arbitrarily increased from 0.49 to 0.6 fm in order to fit the experimentally observed peak positions. One objective of the present work is to remove this ambiguity in the optical-model parameters of the exit channel.

Most of the transitions studied in Refs. 1 and 2 led to final states having angular momentum $j_f = j_> = l_f + \frac{1}{2}$ and the normalizations of the angular distributions for them were satisfactory. There was agreement between the relative spectroscopic factors derived from $(^3He, d)$ and $(^{16}O, ^{15}N)$ reactions; absolute normalizations in the latter reaction were too high by factors ranging from 1.0 to 3.5, but this was not considered serious because the calculated cross sections were so very sensitive to the bound-state parameters.

Recently, however, other groups[5,7] have noticed a consistent discrepancy between the predictions of no-recoil calculations and the experimentally observed relative cross sections for transitions to $j_> = l_f + \frac{1}{2}$ and $j_< = l_f - \frac{1}{2}$ final states. This has been observed at energies comparable to the Coulomb barrier as well as at much higher energies, and for both ^{16}O and ^{12}C projectiles. In the $(^{16}O, ^{15}N)$ reaction, the spectroscopic factors are correct for transitions to $j_>$ states; but for transitions to $j_<$ states, they are too large by factors of up to 8. Calculations by Nagarajan[8] and by DeVries and Kubo[9] show that this j dependence might be explained in terms of recoil effects neglected in the calculations of Refs. 5 and 7, i.e., in terms of the change in the distance between the center of mass of the projectile and that of the nucleus when the transferred particle is thought of as being first a part of the former and then a part of the latter. References 8 and 9 both predict that the recoil effect should increase with increasing projectile energy, and that in the $(^{16}O, ^{15}N)$ reaction the effect should be relatively more important for transitions to $j_<$ final states than for those to $j_>$ final states.

To investigate these points, we have studied the $^{88}Sr(^{16}O, ^{15}N)^{89}Y$ reaction for a range of bombarding energies; data obtained simultaneously for other transfer reactions will not be discussed here. Elastic scattering angular distributions for ^{16}O on ^{88}Sr and for ^{15}N on ^{89}Y have been analyzed to yield optical-model parameters in the entrance and exit channels, respectively. These optical potentials are used in the calculation of

the one-nucleon transfer angular distributions, which are compared with the data to see whether a consistent fit can be obtained as the incident energy is varied from below the Coulomb barrier to above it. Since ^{88}Sr has a good closed subshell for protons,[10] the ^{88}Sr(^{16}O, ^{15}N) reaction leads to good single-particle states in ^{89}Y, the $2p_{1/2}$ and $1g_{9/2}$ states. The observed energy dependence of the magnitudes of the cross sections to these states (which have angular momenta of $j_<$ and $j_>$, respectively) indicates the increasing importance of recoil contributions at higher incident energies.[11]

The use of ^{88}Sr as target has the additional advantage that the inelastic scattering of ^{16}O to the 2^+ first excited state at 1.84 MeV excitation in ^{88}Sr can be studied with complete separation between the elastically and inelastically scattered particles.

Experimental details are given in Sec. II. Optical-model fits to the elastic scattering data in the entrance and exit channels are discussed in Sec. III, in which inelastic scattering data are also presented. The one-proton transfer angular distributions and no-recoil DWBA fits to them are discussed in Sec. IV, and a semiclassical treatment of the data is given in Sec. V.

II. EXPERIMENTAL DETAILS

The experiment was performed with ^{16}O beams of 44.0, 46.0, 48.0, 52.0, 56.0, and 59.0 MeV from the Argonne FN tandem accelerator. Beam currents of 100–200 nA bombarded targets of isotopically enriched ^{88}Sr evaporated onto 30-μg/cm^2 carbon backing to a thickness of 30–80 μg/cm^2. The emerging particles were detected and identified by up to four ΔE-E counter telescopes mounted on the computer-controlled arm of a 70-in. scattering chamber.[12] After pulse multiplication and addition, the resulting mass and energy signals were stored in four 64×256-channel arrays of the 64 000 word external memory of an ASI-210 on-line computer. The multipurpose program SCATTERDAM-5[13] was used to collect the data.

The outgoing particles detected were ^{16}O, ^{15}N, ^{14}C, and ^{12}C. The ΔE detectors used were about 10 μm thick, and the lower limit of 44 MeV for the bombarding energy was fixed by the requirement that the outgoing particles (which for the transfer channels were peaked at back angles) had to have sufficient energy to penetrate this thickness. The upper limit of 59 MeV was fixed by the terminal voltage of the tandem.

Target thicknesses and solid angles were adjusted to get the highest possible yield and resolution for the range of incident energies covered. At the lower energies, at which the angles of interest were the back angles, reflected particles had to be used, whereas transmitted particles were used at the higher energies. To keep the resolution constant, the target thickness was halved for the lower energies, since the resolution was limited primarily by target thickness. The resulting reduction of yield at the lower energies was partially compensated for by using wider slits (up to 0.9 msr); this could be done because the kinematic spread in energy due to spread in angle is least at 180° (and maximum at 90°). Figure 1 shows the spectrum of emerging ^{15}N ions for a bombarding energy of 48 MeV; the energy resolution of ~400 keV full width at half maximum (FWHM) was enough to completely separate the ground state of ^{89}Y from the first excited state at 0.91 MeV.

The angular distribution of ^{15}N elastically scattered from a self-supporting ^{89}Y target 250 μg/cm^2 thick was obtained for an incident energy of 49.5 MeV, which is the energy of the emerging ^{15}N ion in the reaction ^{88}Sr(^{16}O, ^{15}N)^{89}Y$_{g.s.}$ at a bombarding energy of 56 MeV.

Absolute cross sections were obtained by normalizing the reaction data to the elastic scattering,

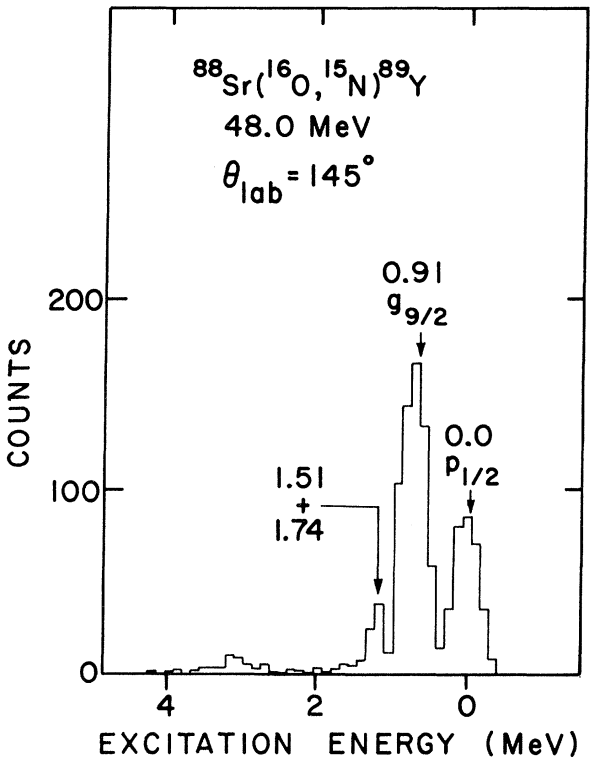

FIG. 1. Energy spectra for the outgoing ^{15}N particles from transfer reactions resulting from 48.0-MeV ^{16}O ions incident on a ^{88}Sr target.

which was pure Rutherford scattering at forward angles. This procedure eliminated errors due to the possible variation in the charge state of the outgoing ^{16}O ions with bombarding energy. The absolute cross sections for the one-proton transfer reaction are estimated to be accurated to within 15%. Nair, Blair, and Reisdorf[14] have measured the excitation function for the $^{88}Sr(^{16}O, ^{15}N)$ reaction at $\theta_{lab} = 170°$ for incident ^{16}O energies from 42.5 to 50 MeV. Their measured cross sections agree within the quoted error with the values we get at 44-, 46-, and 48-MeV incident energies.

III. ELASTIC SCATTERING

Elastic scattering data for $^{16}O + ^{88}Sr$ were obtained simultaneously with the transfer data at all the bombarding energies used. Since it is not feasible to display all the angular distributions obtained on a single plot with the scattering angle as the abscissa, Fig. 2 shows instead the ratios of the elastic to the Rutherford cross section plotted against the distance of closest approach $D(\theta)$ for a pure Coulomb field, this distance being given by

$$D(\theta) = (Z_1 Z_2 e^2 / 2E_{c.m.})(1 + \csc \tfrac{1}{2}\theta). \quad (1)$$

On this plot, the data points taken at all energies and angles fall on one universal curve, which may be approximately parametrized[3] as

$$\sigma/\sigma_R = \begin{cases} 1 & \text{for } D \geq D_0 \\ \exp[(D - D_0)/\Delta] & \text{for } D < D_0 \end{cases}.$$

This expression takes no account of the rise in σ/σ_R that occurs just before the decrease sets in and is typical of Fresnel diffraction phenomena.[15] The decrease from the Rutherford cross section is due to nuclear interaction; it begins when the distance of closest approach decreases to $D_0 \approx 11.3$ fm, which may also be written as $D_0 \approx 1.62(A_1^{1/3} + A_2^{1/3})$ fm, where A_1 and A_2 are the mass numbers of projectile and target, respectively. This value of D_0 corresponds to a Coulomb barrier of 39 MeV for the $(^{16}O + ^{88}Sr)$ system and hence to a laboratory energy of 46 MeV for ^{16}O ions. The $1/e$ length Δ for the exponential fall off has a value of 0.4 fm. Christensen *et al.*[3] have shown that a semiclassical treatment gives $\Delta = \frac{3}{4}a$, where a is the diffuseness of the imaginary part of the corresponding Woods-Saxon potential. The value $a = 0.5$ fm would give the observed value of Δ. The $^{15}N + ^{89}Y$ elastic scattering data at 49.5 MeV also fall on the curve shown in Fig. 2.

The optical-model fits to the $^{16}O + ^{88}Sr$ and $^{15}N + ^{89}Y$ elastic scattering data at 56 and 49.5 MeV, respectively, are shown in Fig. 3. The optical-

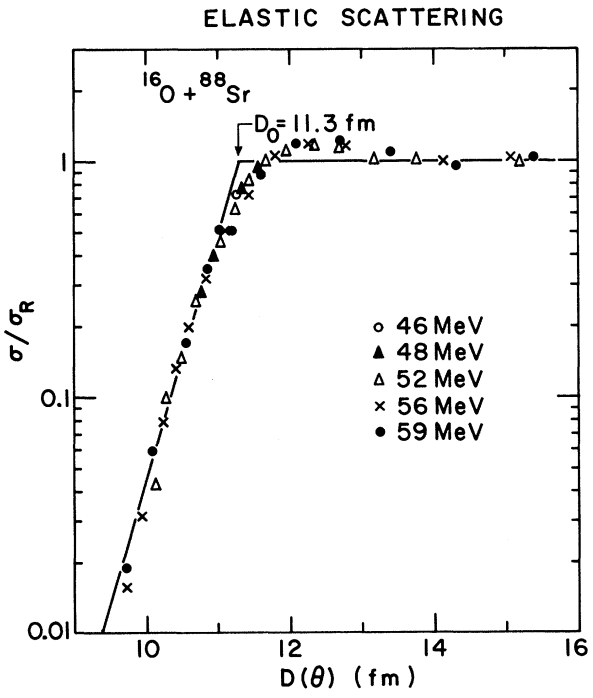

FIG. 2. Elastic scattering cross section, expressed as the ratio to the Rutherford value, for ^{16}O ions striking ^{88}Sr at various incident energies. The abscissa $D(\theta)$ is the distance of closest approach.

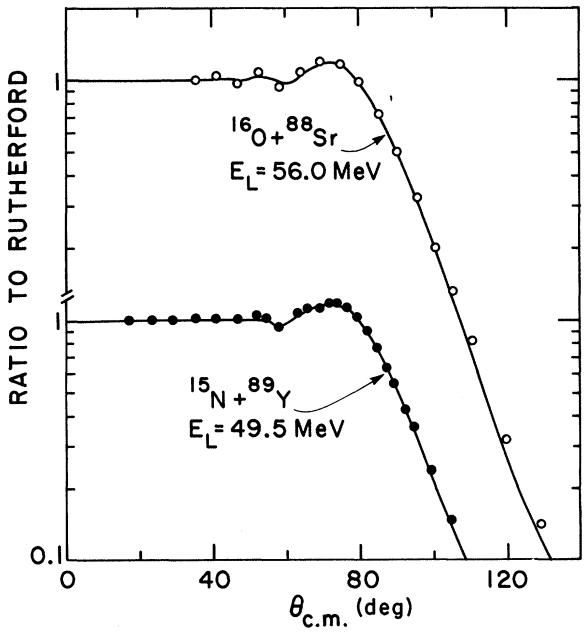

FIG. 3. Angular distributions for ^{16}O elastically scattered on ^{88}Sr and for ^{15}N on ^{89}Y. The solid curves are fits with optical-model set I.

TABLE I. Optical-model parameters for the potential $U=-(V+iW)\{1+\exp[(r-R)/a]\}^{-1}$ by use of the ABACUS search routine.

Projectile	Parameter set	V (MeV)	W (MeV)	R (fm)	a (fm)	r_0 (fm)	χ^2
^{16}O	I	100	25	8.44	0.5	1.21	1.9[a]
	II	600	15.2	8.93	0.3	1.28	3.8[a]
	III	300	60.6	7.89	0.5	1.13	2.0[a]
^{15}N	I	100	25	8.44	0.5	1.22	2.0[b]

[a] Done at $E_{lab}=56.0$ MeV.
[b] Done at $E_{lab}=49.5$ MeV.

model potential had the form

$$U(r)=V_R(r)+iW_I(r)+V_C(r),$$

where

$$V_R(r)=V_R\{1+\exp[(r-R_R)/a_R]\}^{-1},$$
$$W_I(r)=W_I\{1+\exp[(r-R_I)/a_I]\}^{-1}.$$

The Coulomb potential $V_C(r)$ was taken to be that due to a uniformly charged sphere of radius R_R. The optical-model parameters were obtained by use of the search routine of the program ABACUS.[16] One really has very little to fit: the only parameters are the angle at which the break from the Rutherford scattering occurs and the slope of the fall off. So the radii of the real and imaginary wells and also of the real and imaginary diffusenesses were constrained to be equal—i.e., $R_R=R_I$ and $a_R=a_I$. Even this was not enough to give a unique potential, as shown in Table I: potential sets I, II, and III all gave good fits, with the indicated values of χ^2. Set I has been found to work well for fp-shell nuclei also—e.g., in the elastic scattering of ^{16}O on the Ca nuclei.[17] Becchetti *et al.*[18] have found parameters by fitting data for 60-MeV ^{16}O on targets of Ca to Zr; these parameters do not fit the present data well. Our potential set I gave excellent fits to the 56- and 59-MeV elastic scattering data and a good fit to the 52-MeV data, but the strength of the imaginary potential had to be slightly decreased in order to fit the 48-MeV data.

Our purpose in determining these potentials was not to investigate the parameters of the optical model as such in detail, but rather to see whether they could be used to obtain the necessary distortions in fitting the transfer data. That potential sets I, II, and III all fit the elastic scattering data equally well is shown in Fig. 4, which displays the calculated transmission coefficients as a function of the orbital angular momentum brought in by the incident ion; the three potentials give nearly identical transmission coefficients. In particular, the critical angular momentum, defined as that for which $T(l)=0.5$, is about $l=23$ at 56 MeV. The three potentials are similar outside the nucleus but differ widely from each other in the nuclear interior. Thus the elastic scattering determines only the far tail of the optical potential. It is expected (and verified in Sec. IV) that the one-nucleon transfer is a surface-dominated reaction, and therefore the details of the interaction in the interior region should not matter for describing it.

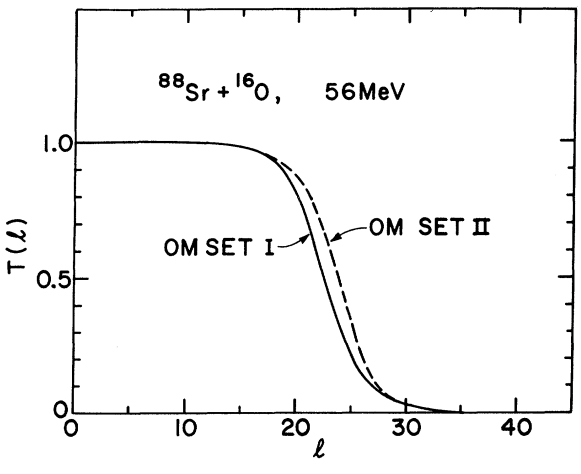

FIG. 4. Transmission coefficients $T(l)$ for the scattering of ^{16}O from ^{88}Sr, calculated with the optical-model potentials given in Table I and plotted against the orbital angular momentum brought in by the ion. The curve for potential set III lies between the curves for sets I and II.

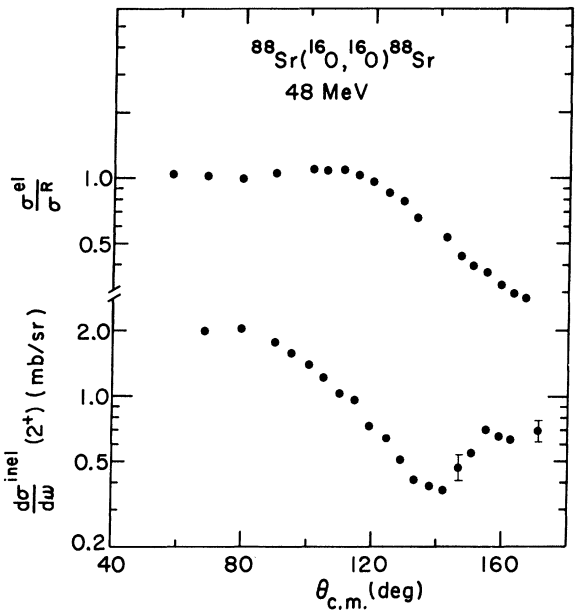

FIG. 5. Angular distributions for the elastic scattering of ^{16}O on ^{88}Sr at 48 MeV, and for the inelastic transition to the 2^+ state of ^{88}Sr.

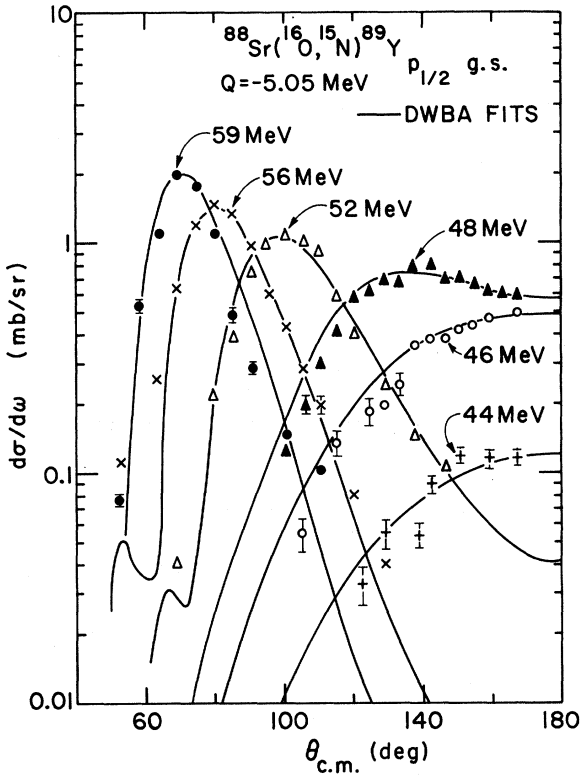

FIG. 6. Experimental and calculated angular distributions for the $^{88}Sr(^{16}O, ^{15}N)$ reaction leading to the $2p_{1/2}$ ground state of ^{89}Y. The bombarding energies are indicated on the curves.

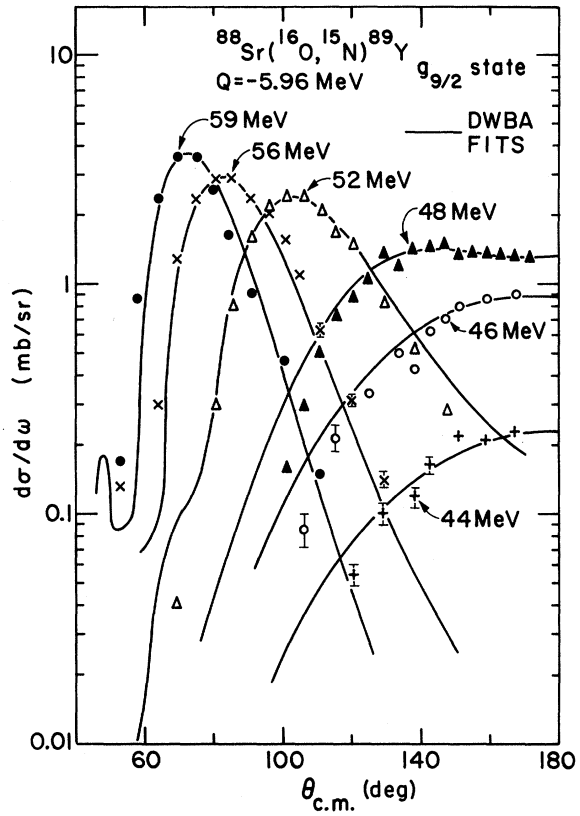

FIG. 7. Same as Fig. 6, but for the $1g_{9/2}$ state of ^{89}Y.

Figure 5 shows the angular distribution for the excitation of the 2^+ state of ^{88}Sr by inelastic scattering of 48-MeV ^{16}O ions. The pronounced minimum in this curve, in the neighborhood of the angle at which the elastic cross section starts deviating from the Rutherford value, has been seen for other nuclei also[19,20] and has been explained as being due to the destructive interference between the Coulomb and the nuclear parts of the inelastic excitation. At higher incident energies, the minimum is found to shift to smaller angles and to become less pronounced. A quantitative analysis was not feasible because the number of partial waves needed was much more than could be handled by the available computer programs.

IV. $^{88}Sr(^{16}O, ^{15}N)$ REACTION

A. Data

By far the strongest states seen in the ^{15}N spectrum (Fig. 1) are the single-particle $2p_{1/2}$ ground state and the $1g_{9/2}$ first excited state of ^{89}Y. No evidence was found for ^{15}N ions going out in excited states nor for strong population of core-excited states in ^{89}Y. The $\frac{3}{2}^-$ state at 1.51 MeV and the $\frac{5}{2}^-$ state at 1.74 MeV in ^{89}Y, which are known[21] to be core-excited states arising from the coupling of the $2p_{1/2}$ proton to the 2^+ state at 1.84 MeV in ^{88}Sr, were populated quite weakly.

Kinematic consideration involving the matching of trajectories for the ingoing and outgoing particles[22] lead to the prediction that at a scattering angle of 180°, the cross section for the one-proton transfer reaction should be maximum at a value $Q = -4.8$ MeV for a bombarding energy of 56 MeV. This value is near to the ground-state value $Q = -5.05$ MeV, and hence the ground state is kinematically favored to have a large cross section, whereas excited states are unfavored. This fact, together with the small spectroscopic factor for the $2d_{5/2}$ state at 3.75 MeV excitation in ^{89}Y, explains why the $\frac{5}{2}^+$ state shows up strongly only at the higher bombarding energies (56 and 59 MeV) and is very weak at 44–52 MeV.

Figure 6 shows the angular distributions for the $2p_{1/2}$ ground state at the various bombarding energies, and Fig. 7 shows them for the $1g_{9/2}$ excited state. The backward-peaked curves at the sub-Coulomb energies (44 and 46 MeV) and the bell-shaped curves at higher energies are well-

known features in heavy-ion transfer reactions[1-3] and have been explained in terms of a semiclassical picture. A comparison of Figs. 6 and 7 shows that the angular distribution at a given energy is insensitive to the transferred orbital angular momentum. This can be explained as follows[23]: Fig. 4 shows that the orbital angular momentum associated with the nuclear surface is ~23 in the entrance channel, and the transfer of a few units of angular momentum can easily be accommodated without much change in the angle θ. The observed scattering angle is therefore primarily determined by the Coulomb deflections of the ingoing and outgoing particles, which are nearly the same for transitions leading to the $p_{1/2}$ and $g_{9/2}$ states because the Q values are almost the same.

Figure 8 shows the angle-integrated cross sections for transitions leading to the $2p_{1/2}$ and $1g_{9/2}$ states of ^{89}Y at various bombarding energies, and indicates that excitation functions below the barrier cannot be used for the determination of the transferred L any more than the angular distributions can be. The figure also shows the total cross sections for the (^{16}O, ^{15}N) and (^{16}O, C) reactions, summed over all final states. It is clear, first, that once the incident energy is sufficiently high for the ions to overcome the Coulomb barrier, there is little further increase in the cross section and, second, that the cross section for four-nucleon transfer becomes significant at a higher incident energy—and hence at a closer distance of approach—than that for the one-nucleon transfer.

B. DWBA Analysis

Distorted-wave calculations for the reaction were done by use of the no-recoil finite-range code RDRC of Schmittroth, Tobocman, and Golestaneh,[6] modified to treat 100 partial waves. This code treats finite-range effects by expanding the form factors of the projectile and final heavy nucleus in a harmonic-oscillator basis. The interaction used was of the "post" form, which is appropriate since the binding of the transferred proton is stronger in the (^{15}N+p) system than in the(^{88}Sr+p) system. The set I optical-model parameters dicussed in Sec. III were used. Bound-state parameters for the ^{88}Sr+p system were those used in the analysis of ^{88}Sr(^{3}He, d) reaction[10]; the parameters for the ^{15}N+p system were those used in an analysis of the ^{208}Pb(^{16}O, ^{15}N) reaction.[24] These parameters are listed in Table II.

Table III shows the relevant reaction quantum numbers for transitions to the $2p_{1/2}$, $1g_{9/2}$, and $2d_{5/2}$ states of ^{89}Y. For the transition from the single-particle state (l_1, j_1) to the state (l_2, j_2),

TABLE II. Bound-state parameters.

System	R_0 (fm)	a (fm)	V_{so} (MeV)	Ref.
^{15}N+p	1.20	0.60	7	24
^{88}Sr+p	1.20	0.65	7	10

the selection rules on the orbital angular momentum transfer L are

$$|l_1 - l_2| \leq L \leq (l_1 + l_2) ,$$

$$|j_1 - j_2| \leq L \leq (j_1 + j_2) ,$$

$$(-1)^{l_1 + l_2} = (-1)^L .$$

The first rule holds only if there is no spin-orbit term in the optical-model potential, the second is exact, and the last holds only if one ignores recoil. Application of these rules leads to the transfer L values given in Table III.

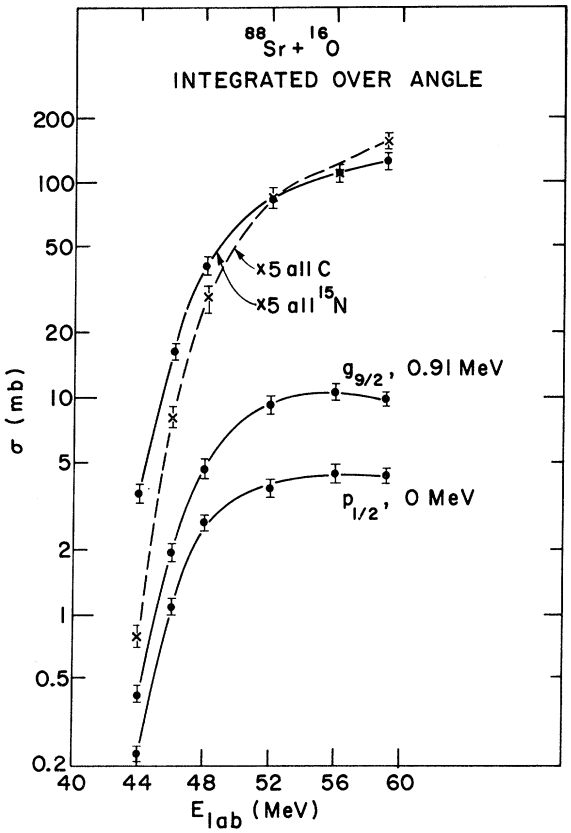

FIG. 8. Angle-integrated cross sections for ^{88}Sr + ^{16}O reactions as a function of the laboratory bombarding energy. In the top two curves the cross sections have been summed over all final states for outgoing particles of ^{15}N and all C; the lower two curves are for the reaction ^{88}Sr(^{16}O, ^{15}N) leading to the $2p_{1/2}$ and $1g_{9/2}$ states of ^{89}Y. The curves are drawn just to guide the eye.

TABLE III. Reaction quantum numbers for ^{88}Sr-(^{16}O, ^{15}N) transitions to the indicated states of ^{89}Y. The spectroscopic factor $(C^2S)_2$ in the last column was obtained from the work on ^{88}Sr(^{3}He,d), Ref. 10.

Single-particle transition	Excitation (MeV)	L transfer (No recoil)	$(C^2S)_2$ from (^{3}He,d)
$1p_{1/2} \rightarrow 2p_{1/2}$	0	0	0.90
$1p_{1/2} \rightarrow 1g_{9/2}$	0.91	5	0.88
$1p_{1/2} \rightarrow 2d_{5/2}$	3.75	3	0.16

Figures 6 and 7 show the angular distributions calculated by use of optical-model parameters of set I; the fits are very good at all energies. The 44- and 46-MeV angular distributions are unchanged in magnitude and shape when the optical potential is turned off and the Coulomb distortion alone is present. At incident energies of 48 MeV and above, the nuclear potential affects the angular distribution at all angles. The set II optical potential for ^{16}O gave distributions that fitted the data less well, but were nevertheless acceptable.

Figure 9 shows that most of the contribution to the (^{16}O, ^{15}N) reaction comes from a sharply localized region between 10 and 12 fm distant from the center of the ^{88}Sr nucleus. Thus the reaction is confined to the nuclear surface. For comparison, the cross section for the ^{88}Sr(^{3}He, d) reaction is also shown in the figure. On making allowance for the differing radii of ^{16}O and ^{3}He, it is seen that the latter reaction also occurs outside the nuclear surface, though it is much less localized. Thus both the (^{3}He, d) and (^{16}O, ^{15}N) reactions are sensitive only to the tail of the bound-state wave function in the ^{88}Sr $+p$ system and therefore it is reasonable to use the same bound-state parameters in both cases. The fact that the calculated ^{88}Sr(^{16}O, ^{15}N) reaction cross section remains constant up to $R_{co} = 10$ fm means that no cut off is needed to exclude contributions from the nuclear interior. This is a consequence of the strongly absorptive nature of the optical potential used.

The calculated cross section is related to the experimental cross section by the relation

$$(d\sigma/d\Omega)_{\rm exp} = N(C^2S)_1(C^2S)_2(d\sigma/d\Omega)_{\rm RDRC}\,, \qquad (2)$$

where $(C^2S)_1$ and $(C^2S)_2$ are the spectroscopic factors for the projectile system and for the states in the final nucleus. Since the $1p_{1/2}$ single-particle orbit is involved, $(C^2S)_1$ is taken to have the value 2.0; the values for $(C^2S)_2$ are taken from the ^{88}Sr (^{3}He, d) work.[10] The normalization constant N is introduced arbitrarily. Table IV lists the normalization. It is seen that $N(g_{9/2})$ is roughly independent of bombarding energy and that its mean deviation is consistent with the 15% error quoted in Sec. II. In contrast, the normalization for the transitions to the $2p_{1/2}$ state increases with energy. This is clearly shown in Table IV by the ratio $N(p_{1/2})/N(g_{9/2})$, which should be independent of any sytematic error in the determination of absolute cross sections. This energy-dependent discrepancy may be due to neglect of recoil effects in the RDRC calculation.[11] Introduction of recoil would lead to additional values for L: namely $L = 1$ for the $p_{1/2}$ state and $L = 4$ for the $g_{9/2}$ state. The contributions from these additional L values will add on to the contributions from the respective "allowed" L values of 0 and 5 for the two states. Since the calculated cross section increases by a factor of ~3 for every unit increase in L, the recoil effects are relatively more important for the $2p_{1/2}$ state than for the

TABLE IV. Normalization factors N in Eq. (2) which represent the angular distributions for ^{88}Sr(^{16}O, ^{15}N) transitions to the $2p_{1/2}$ and $1g_{9/2}$ states in ^{89}Y.

$E_{\rm lab}$ (^{16}O) (MeV)	$N(g_{9/2})$	$\frac{N(p_{1/2})}{N(g_{9/2})}$
44	1.8	1.03
46	2.6	1.29
48	2.2	1.63
52	2.2	1.63
56	1.9	1.93
59	2.0	2.16
	Average 2.1 ± 0.3	

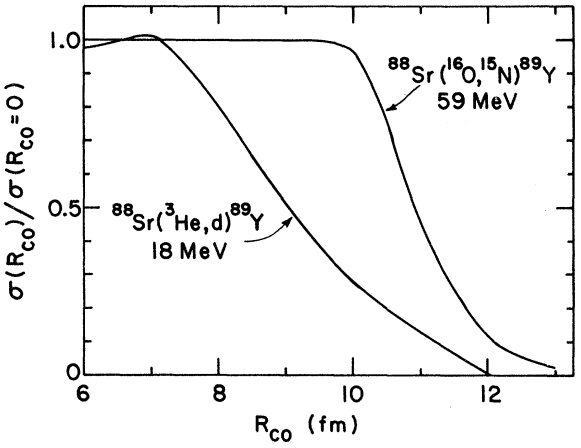

FIG. 9. Calculated cross sections for the ^{88}Sr(^{16}O, ^{15}N) and the ^{88}Sr(^{3}He, d) reactions leading to the ground state of ^{89}Y, plotted as a function of the lower cutoff radius R_{co} in the DWBA integral. The contribution from any particular radius can be inferred from these curves. The half-way radii in the optical potentials for the two reactions, which provide a rough indication of the positions of the nuclear surfaces in the two cases, are at 8.5 and 5.5 fm, respectively.

$1g_{9/2}$ state. Moreover, calculations[8,9] show that recoil effects are more important at higher energies. Both these qualitatively expected features are present in the normalization constants given in Table IV.

Both features—the greater importance of recoil contributions for transitions to $j_<$ final states and the energy dependence—also appear to be present in the data of Ref. 14. At the lower energies, the excitation functions for the ^{140}Ce(^{16}O, ^{15}N), ^{88}Sr(^{16}O, ^{15}N), and ^{140}Ce(^{18}O, ^{17}O) reactions are well fitted with a Buttle-Goldfarb approximation[22] for recoil corrections, whereas calculations for energies above the barrier show a moderate discrepancy, which is greater for the transition to the $p_{1/2}$ state than for that to the $g_{9/2}$ state of ^{89}Y. It is believed that the main source of uncertainty in their analysis[14] is the approximate treatment of recoil.

Figure 10 shows another discrepancy between experiment and the no-recoil calculations. The $2d_{5/2}$ state at 3.75 MeV excitation in ^{89}Y shows up strongly at 56- and 59-MeV incident energies, and the shape and peak position of its angular distribution are identical to those of the distribution of the ground state and of the $g_{9/2}$ state. This is shown in Fig. 10 by the dotted curve, which is a smooth line drawn through the experimental $p_{1/2}$ points. However, the peak of the DWBA angular distribution (solid line), calculated with the same optical parameters that fit the $p_{1/2}$ and $g_{9/2}$ distributions so well, is shifted backward by 8° at 56 MeV; the normalization factor is $N \approx 4.5$. The calculated curve can be made to agree with experiment by changing the diffuseness in both entrance and exit channels from 0.5 to 0.65 fm; but such arbitrary change of parameters has no justification.

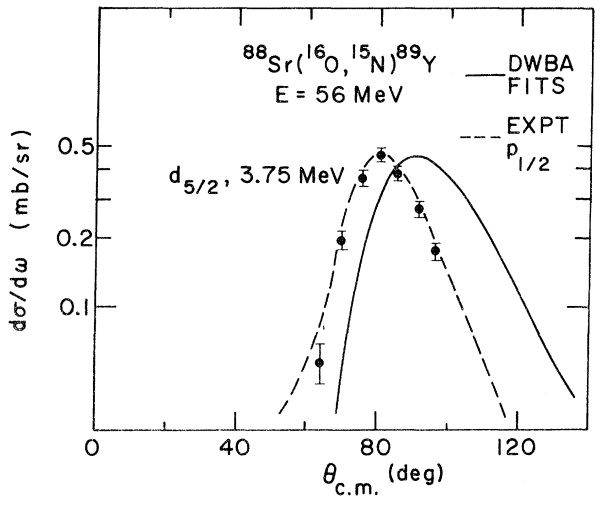

FIG. 10. The experimental angular distribution (points) and the calculated curve (solid line) for the one-proton transfer to the 3.75-MeV excited state in ^{89}Y. The dotted line is a smooth curve drawn through the experimental points for the ground-state transition, measured at the same bombarding energy.

V. SEMICLASSICAL TREATMENT OF THE REACTION ^{88}Sr(^{16}O, ^{15}N)

The transfer probability may be defined through the relation[25]

$$P_{tr} = (d\sigma/d\Omega)_{\text{reaction}}/(d\sigma/d\Omega)_{\text{Rutherford}} ,$$

where division by the Rutherford cross section takes out the phase-space factor. Classically, one may argue[26] that the transfer probability at different energies and angles should depend only on the distance of closest approach $D(\theta)$. This is true at all bombarding energies, but if one uses the pure Coulomb expression (1) for relating D and the scattering angle θ, one is confined to energies below the Coulomb barrier; above the barrier, the relation between D and θ is changed as a result of nuclear distortion. Figure 11 shows that all the $p_{1/2}$ data points at 44-, 46-, and 48-MeV energies do in fact fall

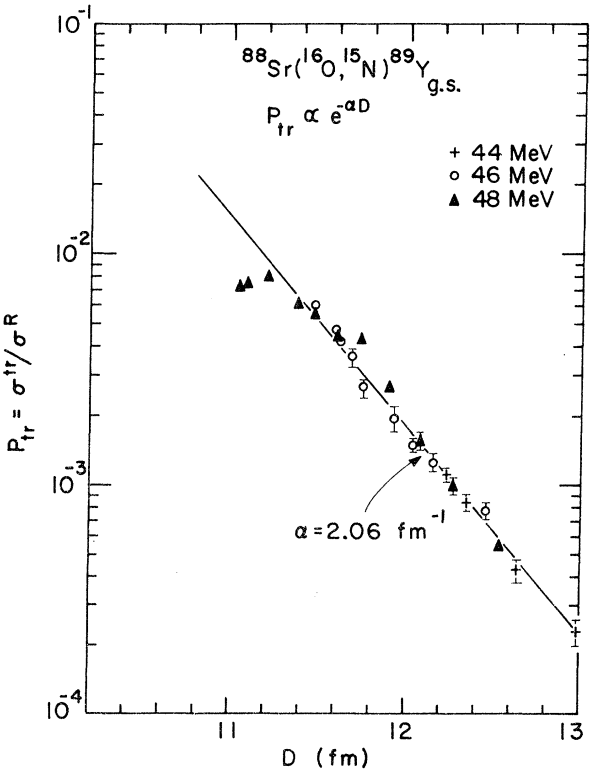

FIG. 11. Semilogarithmic plot of the transfer probability P_{tr} for the $2p_{1/2}$ state vs the distance of closest approach in the entrance channel. Only data for incident energies below the Coulomb barrier are included.

on one smooth exponential curve, down to a distance of about 11.3 fm; below 11.3 fm, the curve rounds off because of nuclear absorption. The $g_{9/2}$ data points fall on a similar curve. The two plots verify the expectation that the probability of transfer should be a simple function of the distance of closest approach for a Coulomb trajectory so long as the center-of-mass energy is less than the barrier energy. This suggests that some theory much less elaborate than DWBA is enough for treating the sub-Coulomb transfer reaction—namely, a theory that treats the reaction as a small perturbation on predominantly Rutherford scattering. Such a semiclassical theory would avoid the main limitation of DWBA calculations—the necessity of having a very large number of partial waves.

The transfer probability can be written as

$$P_{\mathrm{tr}} \propto \exp(-\alpha D).$$

The value of α from the sub-Coulomb $p_{1/2}$ data points is $\sim 2.06\ \mathrm{fm}^{-1}$. The magnitude of α is expected to be related to the slopes of the bound-state wave functions of the transferred particle in the projectile and in the final nucleus, although it is not equal to either of them.

VI. SUMMARY AND CONCLUSIONS

The main conclusions of the present work are the following.

(a) Elastic scattering and one-nucleon transfer appear to be consistently described by the optical model and DWBA, as long as the Q mismatch is not too large.

(b) The angular distributions in Coulomb-dominated one-nucleon transfer reactions are insensitive to small differences in the transferred orbital angular momentum. This precludes the use of the angular distribution to determine the spin of the final state and to detect "forbidden" L contributions brought in by the full recoil treatment.

(c) In the case of the $(^{16}O, ^{15}N)$ reaction, transitions to $j_>$ states are reasonably well described by no-recoil DWBA calculations, whereas transitions to $j_<$ states show discrepancies. The existence of such a j dependence appears to be well established[27] but a quantitative treatment including recoil is still lacking. The energy dependence of the recoil contributions is evident from the data.

At the present time, there exist no DWBA programs that can do the full finite-range calculation in a reasonable amount of computing time. Once such programs become available, it is hoped that the present data would provide a testing ground of the theory.

ACKNOWLEDGMENTS

I wish to thank my advisor, John Schiffer, for making available the facilities of Argonne National Laboratory and for much invaluable advice, support, and encouragement. I gratefully acknowledge the help of K. Katori and H. J. Körner during data taking, and I thank them and G. C. Morrison for valuable discussions during data analysis. J. Kulaga helped introduce me to the details of performing the RDRC calculations. The operating crew of the tandem were very helpful in providing good beams.

Note added in proof: The incident energies quoted are nominal accelerator energies, the actual effective energies are lower by (200–300 keV) because of the effects of target thickness and a slight error in the calibration of the analyzing magnet. The 44-MeV transfer data are most affected by this, because of the sharp energy dependence of the cross section. It is expected that this would raise the value of $N(g_{9/2})$ in Table IV to ~2.1. The ratio of normalization factors is not altered. A finite-range DWBA calculation including recoil *has* been done very recently by Tamura and Low,[28] who communicated their results to us after the present article was completed. They find[11] that the energy dependence of $N(p_{1/2})$ almost disappears with their exact calculation, in agreement with our expectation stated above.

---

*Work performed under the auspices of the U. S. Atomic Energy Commission.

†Presented as a thesis to the Department of Physics, The University of Chicago, in partial fulfillment of the requirements for a Ph.D. degree.

‡Present address: Nuclear Structure Research Laboratory, University of Rochester, Rochester, New York 14627.

[1]H. J. Körner, G. C. Morrison, L. R. Greenwood, and R. H. Siemssen, Phys. Rev. C 7, 107 (1973).

[2]J. V. Maher, K. A. Erb, and R. W. Miller, Phys. Rev. C 7, 651 (1973).

[3]P. R. Christensen, V. I. Manko, F. D. Becchetti, and R. J. Nickles, Nucl. Phys. A207, 33 (1973).

[4]D. K. Scott, P. N. Hudson, P. S. Fisher, C. U. Cardinal, N. Anyas-Weiss, A. D. Panagiotou, P. J. Ellis, and B. Buck, Phys. Rev. Lett. 28, 1659 (1972).

[5]D. G. Kovar, F. D. Becchetti, B. G. Harvey, F. Pühlhofer, J. Mahoney, D. W. Miller, and M. S. Zisman, Phys. Rev. Lett. 29, 1023 (1972).

[6]F. Schmittroth, W. Tobocman, and A. A. Golestaneh, Phys. Rev. C 1, 377 (1970).

[7]F. D. Becchetti, P. R. Christensen, V. I. Manko, and R. J. Nickles, Phys. Lett. 43B, 279 (1973)
[8]M. A. Nagarajan, Nucl. Phys. A196, 34 (1972).
[9]R. M. DeVries and K. I. Kubo, Phys. Rev. Lett. 30, 325 (1973).
[10]J. Picard and G. Bassani, Nucl. Phys. A131, 636 (1969).
[11]N. Anantaraman, K. Katori, and H. J. Körner, Phys. Lett. 46B, 67 (1973).
[12]R. H. Siemssen, H. T. Fortune, J. W. Tippie, and J. L. Yntema, in *Nuclear Reactions Induced by Heavy Ions*, edited by R. Bock and W. Hering (North-Holland, Amsterdam, 1970), p. 174.
[13]J. W. Tippie, IEEE Trans. Nucl. Sci. NS-19, 645 (1972).
[14]K. G. Nair, J. S. Blair, W. Reisdorf, W. R. Wharton, W. J. Braithwaite, and M. K. Mehta, Phys. Rev. C 8, 1129 (1973).
[15]W. E. Frahn and R. H. Venter, Nucl. Phys. 59, 651 (1964).
[16]E. H. Auerbach, Brookhaven National Laboratory Report No. BNL-6562, 1962 (unpublished); revised by S. Zawadzki.
[17]K. O. Groeneveld, L. Meyer-Schützmeister, A. Richter, and U. Strohbusch, Phys. Rev. C 6, 805 (1972).
[18]F. D. Becchetti, P. R. Christensen, V. I. Manko, and R. J. Nickles, Nucl. Phys. A203, 1 (1973).
[19]F. Videbaek, I. Chernov, P. R. Christensen, and E. E. Gross, Phys. Rev. Lett. 28, 1072 (1972).
[20]F. D. Becchetti, D. G. Kovar, B. G. Harvey, J. Mahoney, B. Mayer, and F. G. Pühlhofer, to be published.
[21]J. Alster, D. C. Shreve, and R. J. Peterson, Phys. Rev. 144, 999 (1966).
[22]P. J. A. Buttle and L. J. B. Goldfarb, Nucl. Phys. A176, 299 (1971).
[23]G. C. Morrison, J. Phys. (Paris) Suppl. 33, C5-111 (1972).
[24]A. R. Barnett, W. R. Phillips, P. J. A. Buttle, and L. J. B. Goldfarb, Nucl. Phys. A176, 321 (1971).
[25]G. Breit and M. E. Ebel, Phys. Rev. 103, 679 (1956).
[26]K. R. Greider, Ann. Rev. Nucl. Sci. 15, 291 (1965).
[27]D. Kovar, Argonne National Laboratory Physics Department Informal Report No. PHY-1973B, 1973 (unpublished).
[28]T. Tamura and K. S. Low, private communication and to be published.